Observation and analysis of the ν_3 band of NH_3^+

M. G. Bawendi,[a] B. D. Rehfuss, B. M. Dinelli,[b] M. Okumura, and T. Oka
The Department of Chemistry and The Department of Astronomy and Astrophysics, The University of Chicago, Chicago, Illinois 60637

(Received 14 September 1988; accepted 3 January 1989)

The ν_3 degenerate vibration–rotation band of the ammonia cation NH_3^+ was observed and analyzed. The spectrum was detected in direct absorption using a tunable difference frequency spectrometer combined with velocity modulation. The ion was produced in a 6 kHz ac discharge with a gas mixture of $He:H_2:NH_3$ ($\sim$250:8:1) and with a total pressure of $\sim$6 Torr. Spin–rotation splittings for most Q-branch transitions were well resolved and spin–rotation interaction constants were determined. A symmetric rotor Hamiltonian with A_1–A_2 splittings and l resonance was used to analyze the spectrum. The spectral pattern indicates that NH_3^+ is a planar molecular with D_{3h} symmetry, consistent with a $^2A_2''$ ground electronic state.

INTRODUCTION

The past decade has been an explosion in the number of high resolution spectroscopic studies of molecular ions, especially those containing C–H, N–H, and O–H stretching modes. Among such ions already studied are the fundamentally important hydroxonium ion (H_3O^+)[1,2] and methyl cation (CH_3^+).[3,4] In this paper we complete the infrared spectroscopic study of the XH_3^+ series (X = C,N,O) with a report on the first observation and analysis of the ν_3 fundamental band of the ammonia cation NH_3^+.

The available structural and quantum mechanical information on NH_3^+ indicates that the ammonia cation is planar with D_{3h} symmetry and a $^2A_2''$ ground electronic state.[5] Douglas and Hollas[6] studied a highly excited electronic state of NH_3 and found it to be planar with D_{3h} symmetry, an observation which suggests a planar or nearly planar cation. The electron spin resonance spectrum of this radical cation confirms its likely planarity.[7] Photoionization experiments by Chupka and Russell[8] and the photoelectron spectroscopy results of Rabalais *et al.*[9] are consistent with a $^2A_2''$ ground state and yield an out-of-plane bending mode ν_2 at $\sim$950 cm^{-1}. *Ab initio* calculations by Lathan *et al.*[10] and Hariharan and Pople[11] also predict a D_{3h} planar structure with an $^2A_2''$ ground electronic state for NH_3^+. Finally, the methyl radical CH_3 which is isoelectronic with NH_3^+ and which was found by Herzberg to have a planar structure,[12] has been recently studied using high resolution infrared spectroscopy[13,14] and a planar structure with D_{3h} symmetry was confirmed.

The high resolution absorption spectrum of the ν_3 band (the in-plane degenerate N–H stretch) of NH_3^+ reported in this paper was recorded with a difference frequency spectrometer combined with velocity modulation detection. The ions were created in an ac discharge. Our results confirm a D_{3h} planar structure for the ammonia cation.

EXPERIMENTAL DETAILS

The absorption spectrum of the ν_3 band of NH_3^+ was observed using a difference frequency spectrometer initially developed by Pine[15] combined with velocity modulation detection.[16] Our difference frequency laser system has been described previously[4] and we only summarize its basic ingredients here. Briefly, tunable infrared radiation was generated by mixing radiation from a fixed frequency argon ion laser with tunable radiation from a ring dye laser in a temperature controlled $LiNbO_3$ crystal. The infrared was split into two beams of equal power, one of which underwent four unidirectional transversals through a discharge cell and the other was used for laser noise subtraction. We estimate a fractional absorption sensitivity of $\sim 5\times10^{-7}$. Ammonia absorptions served as frequency calibrations.

The discharge cell (the "spider") was 1.2 m long with a 12 mm bore. It was air-cooled and contained multiple inlet and outlet ports to maximize the optical path length through the reaction regions. A 6 kHz ac discharge and a current of $\sim$100 mA were used to generate the ions.

Using a mixture of helium, hydrogen, and ammonia, Crofton and Oka[17] observed a number of lines which they could not assign. Many of these lines are now known to be due to NH_3^+ and NH_2^+ absorptions. We found that a $He:H_2:NH_3$ gas mixture of 250:8:1 with a total pressure of $\sim$6 Torr in the cell maximized the population of NH_3^+ in the discharge. Higher pressures of NH_3 resulted in a marked increase in the population of NH_4^+, with a concomitant decrease in signal from NH_3^+ transitions. A number of lines were enhanced with the elimination of hydrogen from the discharge and these were eventually assigned to NH_2^+ transitions.[18] The absence of hydrogen also substantially decreased the NH_3^+ population. Varying the pressures of H_2 and NH_3 thus gave us a chemical basis on which to discriminate between NH_4^+, NH_3^+, and NH_2^+ spectral lines.

The spectral region from 3180 to 3510 cm^{-1} was scanned continuously except for a small gap between 3450–3480 cm^{-1} where the power output of $LiNbO_3$ is low due to OH absorption in the crystal. After assigning the transitions due to NH_3^+ and NH_2^+ fundamental bands, many lines still

[a] AT&T Bell Laboratories, PhD. Scholar.
[b] Present address: Istituto di Spettroscopia Molecolare del C. N. R., Via de' Castagnoli, 1, 40126 Bologna, Italy.

 0021-9606/89/115910-08$02.10

remain unassigned and we suspect that at least some of them belong to hot band transitions of NH_3^+ with the $\nu_2 + \nu_3 \leftarrow \nu_2$ band a possible candidate.

RESULTS AND ANALYSIS

The spectrum observed for NH_3^+ is a typical perpendicular band of an oblate symmetric top molecule. A computer generated stick spectrum of the observed transitions is shown in Fig. 1. The line strengths plotted in Fig. 1 correspond to those experimentally observed. These intensities, which are sensitive to fluctuations in the infrared power and to the slightly different discharge conditions used during our study, yield only a qualitative measure of relative line strengths. The absence of transitions starting from $J =$ odd, $K = 0$ levels in the ground state, together with the absence of any nearby groups of lines clearly indicates a planar structure consistent with a $^2A_2''$ ground electronic state. The approximate 2:1 intensity ratio for $K = 3n$ and $K = 3n \pm 1$ transitions reflects the C_3 symmetry of the molecule. Many spin–rotation splittings in the Q-branch area are well resolved as might be expected from the doublet structure of the ion, and part of a scan exemplifying this splitting is reproduced in Fig. 2. The qualitative features of the spectrum confirm that the ammonia cation has a D_{3h} symmetry, a $^2A_2''$ ground electronic state and is best described by a Hund's case (b) scheme.

Two hundred forty-eight lines were observed and assigned to the ν_3 band of NH_3^+. One hundred twenty-eight of the lines were part of doublets with a splitting ranging from ~ 0.012 to ~ 0.066 cm^{-1}. The spin–rotation splittings were fit separately and hypothetical unsplit values were used to fit the rovibrational transitions. Frequencies and assignments

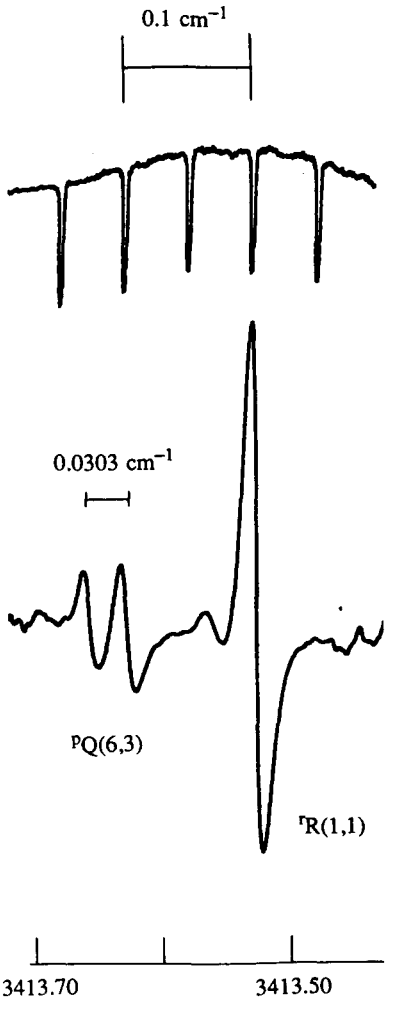

FIG. 2. Example of spin–rotation doubling in the Q branch of the ν_3 band of NH_3^+.

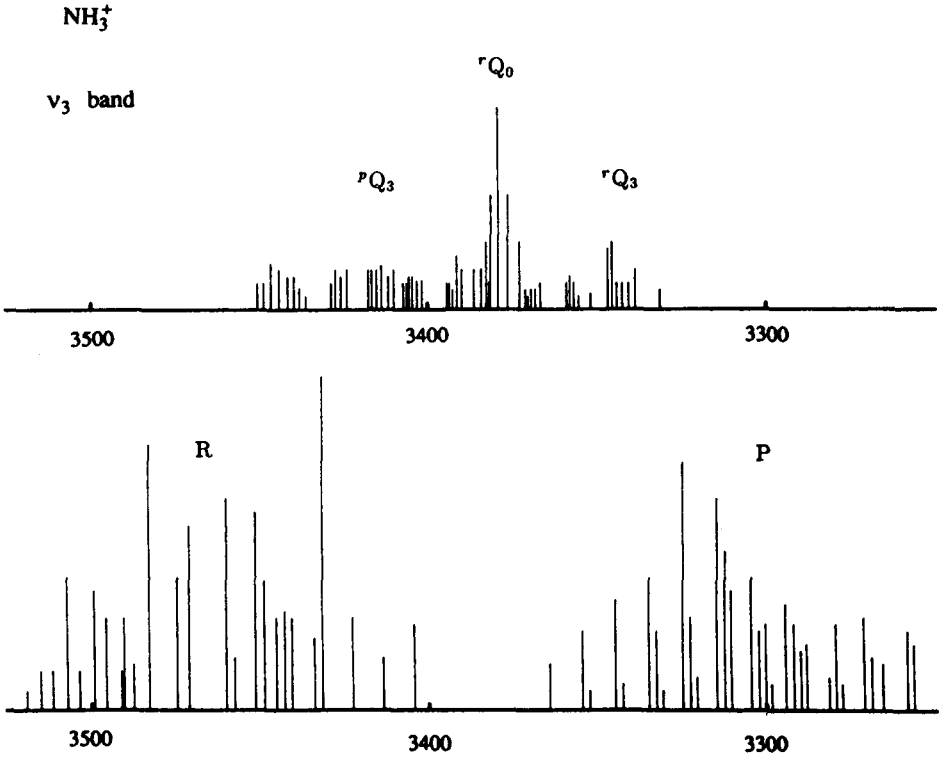

FIG. 1. Computer generated stick diagram of the experimentally observed ν_3 band of NH_3^+.

for these hypothetical unsplit values are listed as "observed" in Table I and spin–rotation splittings are given in Table II. The 184 rovibrational transitions yielded 38 combination differences in the ground state and these are shown in Table III.

Our analysis of the ν_3 band of NH_3^+ follows closely that for the ν_3 bands of CH_3^+[4] and CH_3.[14] The ground state energy levels were of the standard form

$$E(N,K) = BN(N+1) + (C-B)K^2 - D_{NN}N^2(N+1)^2 - D_{NK}N(N+1)K^2 - D_{KK}K^4, \quad (1)$$

where B and C are rotational constants and the D's are quartic centrifugal distortion constants.

The symmetry of the wave functions and the pattern of the rotational energy level diagram are similar to that of CH_3^+ and identical to that of CH_3. In the D_{3h} point group, the total wave function of NH_3^+ must be A_2' or A_2'' in order to obey the Pauli principle, and the nuclear spin wave functions have $4A_1' + 2E'$ symmetry. In NH_3^+ and its isoelectronic partner CH_3, the ground electronic state is $^2A_2''$ and in order to satisfy

$$\Gamma_{elec} \otimes \Gamma_{rot} \otimes \Gamma_{spin} \supset \Gamma_{total} \quad (2)$$

the rotational wave functions must be of A_1', A_1'', E' or E'' symmetry. Since rotational wave functions with A_2' and A_2'' symmetry are forbidden, only J = odd, $K = 0$ levels and one of the A_1–A_2 split levels are allowed. It is important to note that the A_1–A_2 notation originated in the C_{3v} point group where A_1 and A_2 correspond to representations which are symmetric and antisymmetric, respectively, with respect to the σ_v operation.[19] Thus in discussions of A_1–A_2 splittings, A_1' and A_2'' in the D_{3h} point group correspond to A_1 while A_1'' and A_2' correspond to A_2.

The diagonal part of the excited state vibration–rotation Hamiltonian used in our analysis is[4]

$$\begin{aligned} E(\nu_3,N,K,l) = {} & \nu_3 + B'N(N+1) + (C'-B')K^2 \\ & - 2\zeta C'Kl - D'_{NN}N^2(N+1)^2 \\ & - D'_{NK}N(N+1)K^2 - D'_{KK}K^4 \\ & + \eta_N KlN(N+1) + \eta_K K^3 l \\ & + (-1)^{N+1}\delta_{K,1}\delta_{l,1}qN(N+1)/2 \\ & + (-1)^N\delta_{K,2}\delta_{l,-1}\beta_2(N+2)!/(N-2)!, \end{aligned} \quad (3)$$

where ζ is the first order Coriolis coupling constant for the ν_3 degenerate mode and the constants η_N and η_K reflect centrifugal distortion of the Coriolis interaction. The last two terms in Eq. (3) express A_1–A_2 splitting for levels with $|K-l| = 0$ and $|K-l| = 3$, respectively. Since only one of the A_1–A_2 split levels are allowed, the effect of these terms appears as a staggering of the rotational levels. Note that because the electronic ground state is $^2A_2''$ for NH_3^+, the allowed levels are opposite those for CH_3^+ and this is reflected in the factors of $(-1)^{N+1}$ and $(-1)^N$ in Eq. (3).

The term in the Hamiltonian responsible for l-type doubling for levels with $k = l = \pm 1$ also causes l resonance. The off-diagonal matrix element for $K > 1$ is

TABLE I. Observed transitions for the ν_3 fundamental band of NH_3^+ (in cm^{-1}).

N'	K'	l	N''	K''	Obs.	Obs. − Calc.
9	2	1	8	1	3549.798	0.000
12	7	1	11	6	3549.395	0.000
12	8	1	11	7	3539.181	−0.007
9	3	1	8	2	3538.724	0.008
10	5	1	9	4	3535.075	0.006
11	7	1	10	6	3531.873	0.007
9	4	1	8	3	3527.737	0.004
11	8	1	10	7	3521.568	−0.009
12	10	1	11	9	3519.168	0.011
9	5	1	8	4	3516.895	0.005
6	0	−1	5	1	3516.795	−0.004
10	7	1	9	6	3513.931	−0.004
7	2	1	6	1	3512.694	−0.002
11	9	1	10	8	3511.412	−0.002
8	4	1	7	3	3509.234	0.003
13	13	1	12	12	3507.118[a]	−0.564
9	6	1	8	5	3506.186	0.002
10	8	1	9	7	3503.562	−0.004
11	10	1	10	9	3501.114[a]	−0.260
12	12	1	11	11	3499.154[a]	−0.460
5	0	−1	4	1	3497.306	−0.007
9	7	1	8	6	3495.610	−0.003
6	2	1	5	1	3493.559	0.000
10	9	1	9	8	3493.062[a]	−0.260
11	11	1	10	10	3491.075[a]	−0.379
7	4	1	6	3	3490.345	−0.002
8	6	1	7	5	3487.543	−0.007
5	1	1	4	0	3484.877	−0.002
10	10	1	9	9	3482.881[a]	−0.318
8	7	1	7	6	3477.314[a]	0.405
9	9	1	8	8	3474.576[a]	−0.270
6	4	1	5	3	3471.090	−0.008
6	5	1	5	4	3460.104[a]	0.027
7	7	1	6	6	3457.594[a]	−0.248
5	4	1	4	3	3451.510	0.011
6	5	−1	6	6	3450.682	0.002
6	6	1	5	5	3448.880[a]	−0.307
7	5	−1	7	6	3448.741	0.002
8	5	−1	8	6	3446.567[a]	0.023
3	1	1	2	0	3445.314	0.005
9	5	−1	9	6	3444.166[a]	0.062
4	3	1	3	2	3442.812	−0.002
10	5	−1	10	6	3441.552[a]	0.125
5	5	1	4	4	3440.674[a]	0.244
5	4	−1	5	5	3439.736	0.004
6	4	−1	6	5	3438.095	−0.000
7	4	−1	7	5	3436.204	0.001
3	2	1	2	1	3434.038[a]	0.017
4	4	1	3	3	3431.667[a]	0.099
4	3	−1	4	4	3428.679[a]	0.007
5	3	−1	5	4	3427.330	−0.001
6	3	−1	6	4	3425.735	0.000
7	3	−1	7	4	3423.887	−0.004
3	3	1	2	2	3422.626[a]	0.024
3	2	−1	3	3	3417.497	−0.000
4	2	−1	4	3	3416.466[a]	0.004
5	2	−1	5	3	3415.106	0.001
6	2	−1	6	3	3413.645	−0.003
2	2	1	1	1	3413.535	0.002
7	2	−1	7	3	3411.655	−0.007
8	2	−1	8	3	3409.959	0.003
9	2	−1	9	3	3407.173	−0.010
2	1	−1	2	2	3406.221	0.001
3	1	−1	3	2	3405.441	−0.002
4	1	−1	4	2	3404.146	0.003
1	1	1	0	0	3404.314	0.002
5	1	−1	5	2	3403.135	−0.001
11	2	−1	11	3	3401.698	0.009
6	1	−1	6	2	3401.613	−0.004

TABLE I (*continued*).

N'	K'	l	N''	K''	Obs.	Obs. − Calc.
7	1	−1	7	2	3399.864	−0.003
8	1	−1	8	2	3397.889	−0.003
9	1	−1	9	2	3395.693[a]	−0.013
1	0	−1	1	1	3394.819	−0.008
2	0	−1	2	1	3394.314	−0.005
3	0	−1	3	1	3393.557	−0.003
4	0	−1	4	1	3392.546	−0.010
5	0	−1	5	1	3391.309	−0.003
6	0	−1	6	1	3389.837	−0.000
8	0	−1	8	1	3386.233	−0.005
9	0	−1	9	1	3384.133	−0.005
2	1	1	2	0	3382.718	−0.002
10	0	−1	10	1	3381.831[a]	−0.024
4	1	1	4	0	3381.313	−0.006
6	1	1	6	0	3379.162	0.010
8	1	1	8	0	3376.278	0.013
0	0	−1	1	1	3373.794	−0.001
10	1	1	10	0	3372.723	0.004
2	2	1	2	1	3370.986	0.007
3	2	1	3	1	3370.266[a]	0.020
4	2	1	4	1	3369.269	−0.001
12	1	1	12	0	3368.587	−0.008
5	2	1	5	1	3368.057	0.005
6	2	1	6	1	3366.596	−0.000
1	1	−1	2	2	3364.165	−0.002
8	2	1	8	1	3362.986	0.005
3	3	1	3	2	3358.817[a]	0.019
4	3	1	4	2	3357.845	0.002
5	3	1	5	2	3356.651	−0.005
6	3	1	6	2	3355.235	−0.003
2	2	−1	3	3	3354.453	0.008
7	3	1	7	2	3353.659[a]	0.062
1	0	−1	2	1	3352.273	−0.001
8	3	1	8	2	3351.738	0.004
4	4	−1	4	3	3346.626[a]	0.095
5	4	1	5	3	3345.375	0.007
3	3	−1	4	4	3344.630	0.004
6	4	1	6	3	3343.976	−0.005
2	1	−1	3	2	3342.420	0.005
7	4	1	7	3	3342.380	0.006
8	4	1	8	3	3340.561	0.006
1	1	1	2	0	3340.480	−0.001
9	4	1	9	3	3338.527	−0.003
4	4	1	5	5	3334.722	0.008
3	2	−1	4	3	3332.460	−0.001
7	5	1	7	4	3331.248	0.001
2	0	−1	3	1	3330.537	−0.006
5	5	−1	6	6	3324.712	−0.002
4	3	−1	5	4	3322.434	0.007
3	1	−1	4	2	3320.472	−0.000
6	6	−1	7	7	3314.622	−0.003
10	6	1	10	5	3314.380	−0.000
5	4	−1	6	5	3312.300	−0.002
4	2	−1	5	3	3310.328	−0.002
9	7	1	9	6	3305.620	0.001
7	7	−1	8	8	3304.445	−0.008
10	7	1	10	6	3303.517	−0.007
6	5	−1	7	6	3302.092	−0.001
5	3	−1	6	4	3300.077	−0.000
4	1	−1	5	2	3298.358	−0.004
3	1	1	4	0	3296.625	0.001
8	8	−1	9	9	3294.215[a]	0.016
7	6	−1	8	7	3291.795[a]	−0.007
6	4	−1	7	5	3289.765	0.006
5	2	−1	6	3	3287.987	−0.000
8	7	−1	9	8	3281.459[a]	0.027
7	5	−1	8	6	3279.367	0.005
6	3	−1	7	4	3277.606	0.003
9	8	−1	10	9	3271.176[a]	0.188
8	6	−1	9	7	3268.900	0.009
7	4	−1	8	5	3267.108	−0.004
6	2	−1	7	3	3265.671	−0.005
11	11	−1	12	12	3262.666[a]	−0.323
8	5	−1	9	6	3265.579[a]	0.028
7	2	−1	8	3	3242.979	−0.008
9	5	−1	10	6	3233.753[a]	0.061
8	2	−1	9	3	3220.759	0.007

[a] Not included in final fit.

$$\langle N,K+1,l=1|H_{\text{eff}}|N,K-1,l=-1\rangle = \frac{q}{2}\{[N(N+1)-K(K+1)] \times [N(N+1)-K(K-1)]\}^{1/2} \quad (4)$$

and its effect, although not as large as in H_3^+ [20] was found to be important.

Higher order centrifugal distortion constants (H's) and centrifugal distortion contributions to the A_1–A_2 splitting terms (q_N and q_K) improved the standard deviation of the fit somewhat but were not reliably determined and thus not included. A_1–A_2 splittings in the ground state for $K=3$ (h_3) and in the upper state for $K>2$ were found to be negligible.

The standard expression for the spin–rotation splittings of a given rotational level was used

$$\Delta\nu_{\text{SR}} = -(\text{N}+1/2)\,[\epsilon_{bb} - (\epsilon_{bb}-\epsilon_{cc})K^2/N(N+1)]\,. \quad (5)$$

The sign of the ϵ_{bb} constants could not be determined and was assumed to be the same as for CH_3.[14] The effect of including the ϵ_{cc}'s in the fit was negligible and they were set to zero.

Sixty-four data points were fit to the spin–rotation splitting expression [Eq. (5)] using a linear least squares fitting program. The standard deviation of the fit, 0.0018 cm^{-1}, was close to our experimental error of 0.002 cm^{-1}. The ϵ_{bb}'s derived from this fit were used to obtain the hypothetical unsplit values for the rovibrational transitions which are listed as "observed" in Table I. These unsplit rovibrational transitions and the ground state combination differences derived from them were fit simultaneously using a nonlinear least-squares fitting program; the combination differences were given a factor of 3 higher weight. A few transitions whose calculated frequencies deviate markedly from the observed ones were not included in the fit. One hundred fifty-four data points (116 transition frequencies and 38 combination differences) were fit to the energy expressions in Eqs. (3) and (4) with a standard deviation of 0.0052 cm^{-1}. Differences between observed and calculated frequencies are given in Tables I, II, and III and constants determined from the fits appear in Table IV.

The constants for NH_3^+ are very similar to those for CH_3 and CH_3^+, with the only large differences occuring in the l-doubling constant q and the spin–rotation constants ϵ_{bb}. The harmonic part of q is given by[19]

TABLE II. Observed spin–rotation doublings in the ν_3 fundamental band of NH_3^+ (in cm^{-1}).

N'	K'	l	N''	K''	Obs.	Obs. − Calc.
0	0	−1	1	1	0.0275	−0.0026
1	0	−1	2	1	0.0228	−0.0011
2	0	−1	3	1	0.0309	0.0017
4	1	−1	5	2	0.0224	0.0014
6	2	−1	7	3	0.0177	−0.0006
7	2	−1	8	3	0.0211	0.0000
8	2	−1	9	3	0.0271	0.0038
1	1	1	2	0	0.0707	0.0002
3	1	1	4	0	0.0514	−0.0014
2	1	−1	2	2	−0.0496	−0.0000
3	1	−1	3	2	−0.0358	−0.0016
4	1	−1	4	2	−0.0278	−0.0020
5	1	−1	5	2	−0.0212	−0.0007
6	1	−1	6	2	−0.0144	0.0024
3	2	−1	3	3	−0.0588	−0.0009
4	2	−1	4	3	−0.0449	−0.0008
5	2	−1	5	3	−0.0375	−0.0021
6	2	−1	6	3	−0.0303	−0.0010
7	2	−1	7	3	−0.0269	−0.0021
8	2	−1	8	3	−0.0197	0.0016
9	2	−1	9	3	−0.0199	−0.0014
4	3	−1	4	4	−0.0602	0.0023
5	3	−1	5	4	−0.0504	−0.0000
6	3	−1	6	4	−0.0446	−0.0026
7	3	−1	7	4	−0.0337	0.0021
5	4	−1	5	5	−0.0648	0.0007
6	4	−1	6	5	−0.0565	−0.0018
7	4	−1	7	5	−0.0496	−0.0028
6	5	−1	6	6	−0.0663	0.0013
7	5	−1	7	6	−0.0562	0.0017
8	5	−1	8	6	−0.0513	−0.0008
9	5	−1	9	6	−0.0417	0.0029
10	5	−1	10	6	−0.0370	0.0028
2	1	1	2	0	0.0157	−0.0016
2	2	1	2	1	0.0513	0.0009
3	2	1	3	1	0.0327	−0.0031
4	2	1	4	1	0.0285	0.0003
5	2	1	5	1	0.0268	0.0033
6	2	1	6	1	0.0230	0.0026
3	3	1	3	2	0.0604	0.0016
4	3	1	4	2	0.0467	0.0008
5	3	1	5	2	0.0390	0.0011
6	3	1	6	2	0.0310	−0.0016
7	3	1	7	2	0.0297	0.0010
8	3	1	8	2	0.0294	0.0035
4	4	1	4	3	0.0622	−0.0013
5	4	1	5	3	0.0484	−0.0039
6	4	1	6	3	0.0435	−0.0012
7	4	1	7	3	0.0393	0.0001
8	4	1	8	3	0.0362	0.0011
9	4	1	9	3	0.0321	0.0001
7	5	1	7	4	0.0470	−0.0026
10	6	1	10	5	0.0420	−0.0022
9	7	1	9	6	0.0562	−0.0002
10	7	1	10	6	0.0524	0.0009
1	1	1	0	0	−0.0308	−0.0009
3	1	1	2	0	−0.0298	−0.0023
5	1	1	4	0	−0.0329	−0.0017
6	2	1	5	1	−0.0237	−0.0028
7	2	1	6	1	−0.0246	−0.0018
9	4	1	8	3	−0.0118	0.0009
9	3	1	8	2	−0.0200	−0.0016
9	2	1	8	1	−0.0263	−0.0010
5	0	−1	4	1	−0.0458	0.0018

TABLE III. Observed combination differences in the ground state of NH_3^+ (in cm^{-1}).

N_1	N_2	K	Obs.	Obs. − Calc.
4	5	1	105.997	−0.005
5	6	1	126.962	−0.004
0	2	0	63.834	0.003
1	2	1	42.548	−0.005
2	3	2	63.809	0.004
3	4	3	85.041	0.005
2	3	1	63.772	−0.003
3	4	2	84.967	−0.004
4	5	3	106.136	0.004
2	4	0	148.689	0.005
5	6	3	127.115	−0.003
8	9	6	189.989	−0.003
6	7	3	147.965	−0.008
9	10	6	210.415	0.003
5	6	1	126.962	0.000
7	8	3	168.673	−0.002
8	9	3	189.210	0.007
1	2	1	42.546	−0.007
2	3	1	63.776	0.001
2	3	2	63.801	−0.004
3	4	2	84.969	−0.002
4	5	2	106.058	0.007
3	4	3	85.037	0.001
4	5	3	106.138	0.006
5	6	3	127.119	0.001
6	7	3	147.974	0.002
7	8	3	168.676	0.001
8	9	3	189.200	−0.004
4	5	4	106.245	−0.000
5	6	4	127.253	−0.001
6	7	4	148.130	−0.002
5	6	5	127.436	0.006
6	7	5	148.330	−0.006
7	8	5	169.096	0.005
6	7	6	148.590	0.003
7	8	6	169.374	−0.003
8	9	6	189.988	−0.005
9	10	6	210.413	0.001

TABLE IV. Determined molecular constants of NH_3^+.[a]

$\nu_3 - C'_{\zeta 33} - \eta_K/4$	3388.165 5(57)[b]
B'	10.517 93(32)
$C'(1-\zeta_{33}) + \eta_K$	4.675 8(10)
$C' - C'' + 3\eta_K/2$	−0.049 40(52)
D'_{NN}	$0.866\,0(34)\times10^{-3}$
D'_{NK}	$-1.544(14)\times10^{-3}$
$D'_{KK} - \eta_K/4$	$0.567(16)\times10^{-3}$
η_N	$-0.585(47)\times10^{-3}$
B''	10.643 99(22)
D''_{NN}	$0.909\,3(24)\times10^{-3}$
D''_{NK}	$-1.623\,6(98)\times10^{-3}$
$D''_{KK} - D'_{KK}$	$0.049(10)\times10^{-3}$
q	−0.047 85(37)
β_2	$0.040\,1(15)\times10^{-3}$
ϵ_{bb}	−0.039 85(74)
ϵ''_{bb}	−0.040 14(75)

[a] All values are in units of cm^{-1}.
[b] The numbers in parentheses are 3σ.

$$q = \frac{2B^2}{\nu_3}\frac{3\nu_3^2+\nu_2^2}{\nu_3^2-\nu_2^2}\zeta_{23}^2 \quad (6)$$

to yield a predicted value of 0.1227 cm^{-1}. Anharmonic contributions, as in both CH_3 and CH_3^+, must be comparable in magnitude and opposite in sign to make $q = -0.0479$ cm^{-1}. The factor of ~ 4 increase in the spin rotation constants in going from the neutral CH_3 to NH_3^+ is more easily explained. The ϵ_{bb}'s are proportional to the spin–orbit coupling constant[21] which is itself proportional to Z_{eff}/r_{el}^3 where Z_{eff} is the effective charge felt by the unpaired electron and r_{el} is the distance from the central nucleus to the electron. The positive charge on NH_3^+ both increases Z_{eff} and decreases r_{el}, yielding the observed increase in ϵ_{bb}'s.

Rotational selection rules prevent the direct determination of the rotational constants C' and C'' and the centrifugal distortion constants D'_{KK} and D''_{KK} without the observation of forbidden $\Delta|K-l| = 3$ transitions. In order to separate these constants from the observed values of $C' - C''$ and $D''_{KK} - D'_{KK}$, we have used the same inertia defect analysis as Crofton *et al.*[4] for CH_3^+. We do not repeat the details here and present only the final results in Table V.

In order to calculate the inertia defect $\Delta = I_{cc} - I_{aa} - I_{bb}$ and theoretical centrifugal distortion constants, vibrational frequencies for NH_3^+ are needed. The out-of-plane bending mode ν_2 has been reported to be at ~ 950 cm^{-1} in a number of photoelectron spectroscopy[5,9] and photoionization studies.[8,22] To our knowledge, no reliable calculation has been performed to determine the frequencies of the ν_1 and ν_4 modes of NH_3^+. The values chosen in our analysis thus represent appropriately scaled frequencies using the known bands of CH_3 and CH_3^+ and the calculation of DeFrees and McLean[23] on CH_3^+. The approximate vibrational frequencies used in our analysis are $\nu_1 = 3180$ cm^{-1}, $\nu_2 = 950$ cm^{-1}, $\nu_3 = 3390$ cm^{-1}, and $\nu_4 = 1500$ cm^{-1}. A resulting uncertainty of 8% was assumed in the calculation of Δ_0 and the D_{KK}'s. These uncertainties propagate into the calculated constants as given in Table V. The inertia defect of NH_3^+ (0.0461 amu Å^2) is smaller than that of CH_3^+ (0.0578 amu Å^2) due to the larger negative effect of the out of plane bending mode ν_2.

TABLE V. Derived molecular constants of NH_3^+.[a]

ν_3	3388.645 3(63) cm^{-1}
C_0	5.245 7(59) cm^{-1}
C_3	5.195 5(59) cm^{-1}
$C_3\zeta_{33}$	0.520 1(59) cm^{-1}
Δ_0	0.046 1(37) amu Å^2
ζ_{33}	0.100 1(10)
D'_{KK}	$0.694(18)\times10^{-3}$ cm^{-1}
D''_{KK}	$0.743(18)\times10^{-3}$ cm^{-1}
η_K	$0.508(96)\times10^{-3}$ cm^{-1}
r_0	1.0236 Å from B_0
	1.0310 Å from C_0
r_z	1.0304 Å
r_e	1.014 Å[b]

[a] Vibrational frequencies $\nu_1 = 3180$ cm^{-1}, $\nu_2 = 950$ cm^{-1}, $\nu_3 = 3390$ cm^{-1}, and $\nu_4 = 1500$ cm^{-1} obtained as explained in the text were used when necessary.

[b] Predicted *ab initio* value $r_e = 1.012$ Å (Ref. 11).

While most of the observed frequencies in Table I are well fit by the Hamiltonian of Eqs. (1), (3), and (4), as in the study of CH_3^+ a number of transitions deviate markedly from the calculated values. The series in the ^rR branch with $J = K, l = 1$, and $J - 1 = K, l = 1$ form the most conspicuous example. A number of combination differences in the ground state obtained from the ^rR and the ^rQ branch lines agree well with the calculated values and this indicates that the assignments are correct and that the perturbation is in the upper state.

The pattern of the deviations indicates that the perturbing levels are accidentally degenerate with the perturbed levels. The signs of the observed deviations suggest that the vibrational frequency of the perturbing level is less than that of the ν_3 state and that the rotational spacings of the perturbing level are larger than those of the ν_3 state. Although a number of terms may contribute to this perturbation, the most likely candidate appears to be

$$H' = \gamma q_2^2 (q_{3+}q_{4+}J_+^2 + q_{3-}q_{4-}J_-^2) \quad (7)$$

which couples the $2\nu_2 + \nu_4, J, K-1, l = -1$ levels with the $\nu_3, J, K+1, l = 1$ levels. $q_\pm$ and $J_\pm$ in Eq. (7) indicate dimensionless ladder operators for the vibrational and rotational levels, respectively. A least-squares fitting routine using the matrix element

$$\langle 2\nu_2 + \nu_4, J, K-1, l = -1 | H' | \nu_3, J, K+1, l = 1\rangle = \gamma[(J-K+1)(J-K)(J+K)(J+K+1)/2]^{1/2}, \quad (8)$$

and $\Delta E = 2\nu_2 + \nu_4 - \nu_3$, $\Delta B = B_{2\nu_2+\nu_4} - B_{\nu_3}$, and γ as parameters yielded an unacceptably large $\Delta B \sim 0.6$ cm^{-1}, a relatively large $|\gamma| \sim 0.02$ cm^{-1}, but a very reasonable $\Delta E \sim -66$ cm^{-1} which compares well with the value of $+10$ cm^{-1} obtained using the vibrational frequencies listed earlier and in Table V. Each of the constants had a large uncertainty. Because only three constants were allowed to float in the fit and only one perturbing term was taken, the fit is necessarily approximate and the values obtained should thus not be taken too literally.

Since the symmetry of NH_3^+ is D_{3h} from the observed spectrum, the N–H bond length is the only parameter required to fully describe the structure of the ammonia cation. Using C_0 and B_0 we obtain r_0 values of 1.0310 and 1.0236 Å, respectively. These bond lengths are longer than in ammonia where $r_0 = 1.014$ Å.[24] The parameter r_0 corresponds to an effective bond length since it is derived from effective moments of inertia which neglect vibration–rotation interactions. We can determine the zero point[25] N–H bond length r_z (average bond length[26]) according to the method of Ref. 4 where vibration–rotation interactions are included in the calculation of a zero point moment of inertia. We obtain $r_z = 1.0304$ Å. The determination of the equilibrium bond length r_e requires knowledge about the variations of the rotational constants α_s for all four vibrational modes. Since this information is not available experimentally, we estimate the difference between r_z and r_e using the diatomic model

$$r_z - r_e = -\frac{3}{4}\frac{h\nu_1 F_3}{F_2^2}, \quad (9)$$

where the harmonic force constant F_2 and the cubic anhar-

monic force constant F_3 can be estimated using Herschbach and Laurie's empirical formula.[27] We obtain $r_z - r_e = 0.0162$ Å and $r_e = 1.014$ Å which agrees well with the predicted *ab initio* value of 1.012 Å.[11]

PLASMA CHEMISTRY

Our ability to selectively enhance signals from NH_3^+ over those from NH_2^+ and NH_4^+ is, in retrospect, not too surprising. A number of chemical channels are available for the formation and destruction of NH_2^+, NH_3^+, and NH_4^+. These include electron impact dissociative ionization and reactions with metastable He, H_3^+, and NH_3.

The appearance potentials of the electron impact dissociative ionization reactions of ammonia,

$$NH_3 + e \rightarrow NH_3^+ \quad (10)$$
$$\rightarrow NH_2^+ + H + 2e \quad (11)$$
$$\rightarrow NH^+ + H_2 + 2e \quad (12)$$
$$\rightarrow N^+ + H_2 + H + 2e \quad (13)$$

are 10.6, 15.7, 24.3, and ~28 eV, respectively.[28,29] The branching ratio of the reaction of NH_3 with ionized He (which is at a Langevin rate),

$$NH_3 + He^+ \rightarrow NH_3^+ + He \quad (14)$$
$$\rightarrow NH_2^+ + H + He \quad (15)$$
$$\rightarrow NH^+ + H_2 + He \quad (16)$$

has been reported to be 0.08:0.80:0.12.[30] Because of the high ionization potential of He (24.6 eV),[30] the reaction of NH_3 and He^+ thus produces mainly NH_2^+. With H_2 present in the discharge, NH_3^+ is formed by the hydrogen abstraction reactions

$$N^+ + H_2 \rightarrow NH^+ + H, \quad (17)$$
$$NH^+ + H_2 \rightarrow NH_2^+ + H, \quad (18)$$
$$NH_2^+ + H_2 \rightarrow NH_3^+ + H, \quad (19)$$
$$NH_3^+ + H_2 \rightarrow NH_4^+ + H, \quad (20)$$

which have rates of 0.48×10^{-9}, 0.95×10^{-9}, 0.12×10^{-9}, and $\sim3\times10^{-13}$ $cm^3\,s^{-1}$, respectively.[30] For all practical purposes, reaction (20) is so slow as to be negligible. Thus in our discharge, the hydrogen abstraction reactions effectively terminate at NH_3^+.

With H_2 fairly abundant in the discharge, H_3^+ is formed via

$$H_2 + H_2^+ \rightarrow H_3^+ + H. \quad (21)$$

Reaction (21) yields H_3^+ in a distribution of vibrationally excited states, $(H_3^+)^*$,[31] which are deactivated upon collisions with H_2 molecules more efficiently than upon collisions with He. The reactions

$$NH_3 + (H_3^+)^* \rightarrow NH_4^+ + H_2 \quad (22)$$
$$\rightarrow NH_3^+ + H_2 + H \quad (23)$$

occur with a branching ratio of 0.58:0.42.[30] With H_3^+ in the ground state the reaction

$$NH_3 + (H_3^+)^0 \rightarrow NH_4^+ + H_2 \quad (24)$$

produces exclusively NH_4^+.[30]

As the abundance of ammonia is increased in the discharge, the reactions

$$NH_2^+ + NH_3 \rightarrow NH_4^+ + NH \quad (25)$$
$$\rightarrow NH_3^+ + NH_2 \quad (26)$$

with a branching ratio of 0.4:0.6,[30] and the reaction

$$NH_3^+ + NH_3 \rightarrow NH_4^+ + NH_2 \quad (27)$$

become important channels for the destruction of NH_2^+ and NH_3^+ ions.

From the branching ratio of reactions (14)–(16) it is clear that NH_2^+ should dominate over NH_3^+ and NH_4^+ in a He:NH_3 discharge where He is a buffer gas and NH_3 is effectively an impurity. As hydrogen is added to the discharge, reactions (17)–(20) lead to an increase in NH_3^+ concentration and a concomitant decrease in NH_2^+ ions. When a large amount of H_2 is present in the discharge, reactions (22)–(24) yield NH_4^+ which serves as an ion sink and thus prevents NH_2^+ and NH_3^+ from being formed in appreciable quantities. Similarly, as the concentration of NH_3 is increased in the discharge, reactions (25)–(27) decrease the populations of NH_2^+ and NH_3^+ ions in favor of NH_4^+. These results have all been observed experimentally in our discharge. The optimization of the concentration of NH_3^+ thus required a fine-tuning of the discharge conditions. We found that a He:H_2:NH_3 gas mixture with a ratio of 250:8:1 and a total pressure of ~6 Torr maximized the population of NH_3^+ in the discharge.

Ammonia cannot be used as a primary gas in a liquid nitrogen cooled discharge cell since it freezes at the inlet ports. However, a mixture of N_2 and H_2 can effectively replace NH_3 in the discharge. The electron impact ionization reactions

$$N_2 + e \rightarrow N_2^+ + 2e \quad (28)$$
$$\rightarrow N^+ + N + 2e \quad (29)$$

with appearance potentials of 15.6 and 24.4 eV, respectively,[32] and the reaction

$$N_2 + He^+ \rightarrow (N_2^+)^* + He \quad (30)$$
$$\rightarrow N^+ + N + He \quad (31)$$

with a branching ratio of 0.31:0.69,[30] begin the process. The hydrogen abstraction reactions (17)–(20) then yield NH_2^+ and NH_3^+ ions. Ammonia is eventually formed through the electron recombination reaction

$$NH_3^+ + e \rightarrow NH_3 \quad (32)$$

and is deposited on the cell walls as a fine white crystalline powder. Although we were able to observe NH_3^+ in a liquid nitrogen cooled cell, we have found it more convenient to use a water cooled cell almost exclusively to obtain the rotation vibration spectrum of NH_3^+.

ACKNOWLEDGMENT

This work was supported by NSF Grant No. PHY-87-07025.

[1] M. H. Begemann, C. S. Gudeman, J. Pfaff, and R. J. Saykally, Phys. Rev. Lett. **51**, 554(1983).
[2] D. J. Liu and T. Oka, Phys. Rev. Lett. **54**, 1787 (1985).

[3]M. W. Crofton, W. A. Kreiner, M.-F. Jagod, B. D. Rehfuss, and T. Oka, J. Chem. Phys. **83**, 3702 (1985).
[4]M. W. Crofton, M.-F. Jagod, B. D. Rehfuss, W. A. Kreiner, and T. Oka, J. Chem. Phys. **88**, 666 (1988).
[5]G. L. Goodman and J. Berkowitz, *Molecular Ions*, edited by J. Berkowitz and K.-O. Groeneveld (Plenum, New York, 1983), p. 69.
[6]A. E. Douglas and J. M. Hollas, Can. J. Phys. **39**, 479 (1961).
[7]J. S. Hyde and E. S. Freeman, J. Phys. Chem. **65**, 1636 (1961); T. Cole, J. Chem. Phys. **35**, 1169 (1961).
[8]W. A. Chupka and M. E. Russell, J. Chem. Phys. **48**, 1527 (1968).
[9]J. W. Rabalais, L. Karlsson, L. O. Werme, T. Bergmark, and K. Siegbahn, J. Chem. Phys. **58**, 3370 (1972).
[10]W. A. Lathan, W. J. Hehre, L. A. Curtiss, and J. A. Pople, J. Am. Chem. Soc. **93**, 6377 (1971).
[11]P. C. Hariharan and J. A. Pople, Mol. Phys. **27**, 209 (1974).
[12]G. Herzberg, Proc. R. Soc. London Sec. A **262**, 291 (1961).
[13]C. Yamada, E. Hirota, and K. Kawaguchi, J. Chem. Phys. **75**, 5256 (1981).
[14]T. Amamo, P. F. Bernath, C. Yamada, Y. Endo, and E. Hirota, J. Chem. Phys. **77**, 5284 (1982).
[15]A. S. Pine, J. Opt. Soc. Am. **64**, 97 (1976); **66**, 97 (1976).
[16]C. S. Gudeman, M. H. Begemann, J. Pfaff, and R. J. Saykally, Phys. Rev. Lett. **50**, 727 (1983).
[17]M. W. Crofton and T. Oka, J. Chem. Phys. **86**, 5983 (1987).
[18]M. Okumura, B. D. Rehfuss, B. M. Dinelli, M. G. Bawendi, and T. Oka, J. Chem. Phys. **90**, 5918 (1989).
[19]T. Oka, J. Chem. Phys. **47**, 5410 (1967).
[20]T. Oka, Phys. Rev. Lett. **45**, 531 (1980); J. K. G. Watson, S. C. Foster, A. R. W. McKellar, P. F. Bernath, T. Amano, F. S. Pan, M. W. Crofton, R. S. Altman, and T. Oka, Can. J. Phys. **62**, 1875 (1984); J. K. G. Watson, J. Mol. Spectrosc. **103**, 350 (1984).
[21]J. H. Van Vleck, Rev. Mod. Phys. **23**, 213 (1951).
[22]R. J. S. Morrison, W. E. Conaway, T. Ebata, and R. N. Zare, J. Chem. Phys. **84**, 5527 (1986); W. E. Conaway, T. Ebata, and R. N. Zare, *ibid.* **87**, 3447, 3453 (1987).
[23]D. J. DeFrees and A. D. McLean, J. Chem. Phys. **82**, 333 (1985).
[24]G. Herzberg, *Molecular Spectra and Molecular Structure II. Infrared and Raman Spectra of Polyatomic Molecules* (Van Nostrand Reinhold, New York, 1945), p. 439.
[25]T. Oka, J. Phys. Soc. Jpn. **15**, 2274 (1960).
[26]D. R. Herschbach and V. W. Laurie, J. Chem. Phys. **37**, 1668 (1962).
[27]D. R. Herschbach and V. W. Laurie, J. Chem. Phys. **35**, 458 (1961).
[28]A. Crowe and J. W. McConkey, Int. J. Mass Spectrom. Ion Phys. **24**, 181 (1977).
[29]C. E. Brion, A. Hamnett, G. R. Wight, and M. J. Van der Wiel, J. Electron Spectrosc. Relat. Phenom. **12**, 323 (1977).
[30]W. T. Huntress, Jr., Astrophys. J. Suppl. **33**, 495 (1977).
[31]T. Koenig, T. Balle, and W. Snell, J. Am. Chem. Soc. **97**, 662 (1975).
[32]A. Crowe and J. W. McConkey, J. Phys. B **6**, 2108 (1973).